Bima Journal of Science and Technology, Vol. 7 (2) June, 2023 ISSN: 2536-6041

DOI: 10.56892/bima.v7i2.430

DEVELOPMENT OF BENEFICIATED KAOLIN CLAY, SILVER OXIDE AND ZINC OXIDE NANOCOMPOSITE ADSORBENTS TO REMOVE CHEMICAL AND BIOCHEMICAL OXYGEN DEMANDS CONCENTRATION IN DOMESTIC WASTEWTAER

[1]*OGUNDIPE F.O., [2]SAIDU M., [3]ABDULKAREEM A.S. and [2]BUSARI A.O.

[1]Federal Ministry of Water Resources, Abuja, Nigeria
[2]Deaprtment of Civil Engineering, Federal University of Technology, Minna, Nigeria
[3]Department of Chemical Engineering, Federal University of Technology, Minna, Nigeria

*Corresponding Author: ogundipefelixo@yahoo.com

ABSTRACT

This study describes the development of Beneficiated Kaolin Clay (BKC), BKC/Ag, BKC/ZnO and BKC/Ag/ZnO nanocomposite adsorbents produced by blending Silver Oxide (Ag) and Zinc Oxide (ZnO) nanoparticles with kaolin clay for removal of Chemical Oxygen Demand (COD) and Biochemical Oxygen Demand (BOD) concentration from domestic wastewater collected via sewers,High Resolution Transmission Electron Microscope (HRTEM) analysis showed that the produced adsorbents were polycrystalline in nature. The interplanar spacing and average crystalline sizes were 1.775 – 4.712 nm and 26. 834 – 40.258 nm, according to X-Ray Diffractometer (XRD) analysis. The Dispersive X – Ray Fluorescence (XRF) analysis indicated that SiO_2/Al_2O_3 ratios for BKC/Ag, BKC/ZnO and BKC/Ag/ZnO nanocomposites adsorbents were 1.5170, 1.4818 and 1.5231 respectively. Brunauer – Emmett – Teller (BET) analysis showed that the BKC/Ag, BKC/ZnO and BKC/Ag/ZnO had a certain number of macropores ($d > 50$ nm) and a small amount of micropores ($d < 2$ nm) ascribed to mesoporous structures with hysteresis loops of type H3. The COD and BOD concentration removal efficiencies of the produced adsorbents followed this trend:BKC/Ag/ZnO > BKC/Ag > BKC/ZnO > BKC. These adsorbents were excellent in the removal of COD and BOD from domestic wastewater, and hence, recommended for large scale production.

Keywords: Adsorption, Kaolin Clay, COD, BOD, Domestic Wastewater.

INTRODUCTION

Domestic wastewater consists of household waste liquid from toilets, baths, showers, kitchens, sinks and other liquid that is disposed of via sewers (EPA, 2019b; Cigdem, 2010; Hocaoglu *et al*. 2010; Marthe *et al*, 2010). Preliminary investigations of household wastewater in 79 high and middle-income countries showed that 59 % were safely treated (UN Water, 2018). However, in low-income countries such as Nigeria, only 8 % of wastewater undergo treatment of any kind (WWDR, 2017). Wash Norm 2019 showed that only 14 % of the Nigeria populations have access to safely managed drinking water supply services. Increased discharges of domestic wastewater, coupled with agricultural runoff has resulted in the degradation of water in Nigeria (Adewole, 2006).

The key parameter in domestic wastewater is BOD and COD levels (Mutia et al, 2020; Suhendrayatna et al, 2012; Muhammad et al, 2008). COD is a measure of the oxygen equivalent of the organic matter in a wastewater that is susceptible to oxidation by a strong chemical oxidant, such as dichromate. The COD is widely used as a measure of the susceptibility to oxidation of the organic and inorganic materials present in

DOI: 10.56892/bima.v7i2.430

water bodies and a general indication of pollution. BOD is an approximate measure of the amount of biochemically degradable organic matter present in a water sample (Dar, 1999). BOD is usually defined by the amount of oxygen required for the aerobic micro-organisms present in the wastewater to oxidize the organic matter to a stable inorganic form.

Excess organic loads reduce the amount of dissolved oxygen (Idris-Nda *et al*, 2013) in water to critical level and impair the chemical content which can also result into disease such as Cholera, Dysentery, Typhoid, Diarrhoea, Hepatitis and Jaundice (Thyagaraju, 2016). Wastewater with high BOD and COD will decrease oxygen of receiving waterbodies, which in turn can cause death of some organisms and aquatic lives. NESREA 2011 specified maximum permissible limits of 6.0 mg/L and 30 mg/L for BOD and COD of treated effluent in Nigeria. Any values above require treatment before the wastewater can be discharged into the environment in Nigeria.

In an effort to remove COD and BOD from wastewater, conventional anaerobic and aerobic treatments have received greater attention over the past decades due to their numerous advantages such as low energy consumption, low chemical consumption, low sludge production, vast potential of resource recovery, less equipment required and high operational simplicity (Anijiofor*et al*, 2017; Marthe *et al*, 2010; Sylla *et al*, 2018). However, conventional anaerobic and aerobic systems are found to have operational limitations in terms of long Hydraulic Retention Time (HRT), space requirement and facilities to capture biogas (Chan *et al*, 2009). In view of the danger associated to discharge of domestic wastewater with high COD and BOD to receiving rivers and in a bid to protect the environment from further pollution, this research work developed nanocomposite adsorbents by blending Silver Oxide (Ag) and Zinc Oxide (ZnO) nanoparticles with kaolin clay from Kutigi in Niger State, Nigeria to remove COD and BOD from domestic wastewater.

Advances in nanoscale science has shown that many of the current problems in water quality could be resolved by using nanocomposite (Berekaa, 2016; Abdullah *et al*, 2017), bioactive nanoparticles (Sukdeb *et al*, 2007; Thabet *et al*, 2010; Njagi *et al*, 2010; Vikas et al, 2013; Benakashani *et al*, 2016; Shittu and Ikebana, 2017), nanostructured catalytic membranes (Rui *et al*, 2013), nanotubes, magnetic nanoparticles (Ming *et al*, 2012; Sulekha, 2016; Vikas *et al*, 2013), high surface area metal particle (Ralf *et al*, 2011; Sierra *et al*, 2018; Maity et al, 2018) with characteristic length scales of 9-10 nm (Haijiao *et al* 2016). As an environmentally friendly material, nanocomposite adsorbents could efficiently remove heavy metals (Ming *et al*, 2012), Chromium VI (Rui *et al*, 2013), enhance adsorption of lead ion (Yang *et al*, 2008) and use as antibacterial application (Getie S *et al*, 2017b; Haritha *et al*, 2011;Ying *et al*, 2017; Stoyanova *et al*, 2013). However, it wasnoticed that none of the research work reviewed, reported the blend of silver and zinc oxide nanoparticles on kaolin clay support from Kutigi, Niger State, to remove COD and BOD from wastewater collected via household sewers.

Kaolin clay, an aluminosilicate mineral (Yahaya*et al*, 2017; Kuranga *et al* 2018), is classified as potential solid mineral in Nigeria (NBS, 2017). There is deposit of kaolin clay in 13 local government areas of the state namely, Agaie, Bida, Bosso, Edati, Gbako, Katcha, Lapai, Lavun, Mashegu, Mokwa, Paikoro, Shiroro and Wushishi. The kaolin clay minerals are widely utilized for agriculture, ceramics (Auta and Hameed,

DOI: 10.56892/bima.v7i2.430

2013), environmental applications (Murray, 2000), absorbents (Saikia *et al*, 2003; Bachiri et al, 2014) and wastewater treatment (Chun et al, 2013; Cheng *et al*, 2017), production of metakaolin (Kuranga *et al*, 2018; Wilson *et al*, 2017). Attention is on clay materials because of their sheet-like structures that provides high specific surface area (Dhaval & Painter, 2017; Sachin *et al*, 2013; Aroke and Onatola, 2016).

MATERIALS AND METHODS

Materials Collection

Mangifera Indica Leaves for green synthesis of silver and zinc nanoparticles were collected from River Basin Estate, Tundun Fulani, Minna. The kaolin clay was collected from Kutigi, Nigeria. The domestic wastewater was collected via sewer that connected toilets, baths, showers, kitchen and sinks together. Analytical grade chemicals and reagents used in this research work are listed in Table 1.

Table 1: List of Reagents/Chemicals

S/N	Chemical/Reagents	Formula	% Purity	Manufacturer	Uses
1	Silver Nitrate	$AgNO_3$	99.5	BDH Chemicals Ltd., Poole, England	To produce silver nanoparticles
2	Deionised Distilled Water	DDW	0.5 µS/cm	FMWR – NWQRL Minna	*To produce Mangifera Indica leave extract*
3	Zinc Sulphate, (Heptahydrate),	$ZnSO_4.7H_2O$	99	LOBA Chemie, Mumbai, India	To produce Zinc Oxide nanoparticles
4	Zinc Chloride	ZnCl	99.5	J.T Baker Limited, Philipsburg USA	To remove nutrients from raw clay
5	Ethanol	C_2H_5OH	96	EMD Millipore Corporation, Germany	To clean Ag and ZnO nanoparticles
6	Hydrogen Peroxide Solution	H_2O_2	30-32	BDH Chemicals Ltd., Poole, England	To oxide organic matter

Beneficiation of Kaolin Clay

200 g of raw kaolin clay lumps were put in 4 Litres Beakers with 4 Litres of distilled water added. This represents 5 % w/w kaolin clay slurry in distilled water. The Beaker was stirred for 1 hour using Heildolph RGL500 high viscosity stirrer at control speed of 40 revolutions per minute for adequate dispersion in distilled water. The resulting mixture was allowed to swell in distilled water for 22 hrs 57 mins as calculated by Stoke's Law using equation 1.

$$u_s = \frac{g(\rho_p - \rho_w)d_p^2}{18\mu} \quad (1)$$

Where ρ_p = particle density, kg/m^3 (Kaolin clay particle = 1600 kg/m^3), μ = liquid viscosity, kg/m.s (distilled water = 8.90 × 10^{-4} Pa·s), ρ_w = density of water, kg/m^3 (997 kg/m^3), u_s= Particle settling velocity, m/s, d_p = diameter of particle (m), g = acceleration due to gravity, m/s^2(9.81 m/s^2), t = Settling Time, R = particle size (radius) of clay, assumed to be spherical (1µm = 1 X 10^{-6}m), h = Settling Height of Fluid (12 cm = 0.12 m), The resultant slurries were thereafter dried in a laboratory oven at a temperature of 105 ^oC until the water is evaporated and the samples weight became constant. Acid activation was done by treating the beneficiated kaolin clay with 0.5 M of HCl to remove carbonate, washed by 10 % Hydrogen Peroxide (H_2O_2) to oxide organic matter (Bachiri *et al*, 2014) and NaCl to remove nutrients (Cheng *et al*, 2017). The residue from filtration was washed several times with distilled water and monitored until pH 7. The percentage yield

DOI: 10.56892/bima.v7i2.430

(Y) of the beneficiated clay was calculated using equation 2.

$$Y = \frac{Mass\ of\ Purified\ Kaolin\ Clay}{Mass\ of\ Raw\ Kaolin\ Clay}\ x\ 100\% \quad (2)$$

Green Syntheses of ZnO Nanoparticles

10 g of Zinc Sulphate Heptahydrate ($ZnSO_4.7H_2O$) powder was measured and put in 250 mL volumetric flask. DDW was added to 100 mL mark of the volumetric flask. The resultant mixture was stirred using a magnetic stirrer at 150 rpm for 30 minutes. 50 mL volume of the prepared concentration was collected and put in another 100 mL conical flask. The conical flask was put on the hot plate and temperature set to 80 ^oC. *Mangifera Indica* leave (Maity et al, 2018) extract (titrant) was put in a burette, ready for titration. The solution was titrated, while continuously stirred at 80 ^oC until the light-yellow colour was formed (Sierra *et al*, 2018; Daizy, 2010). The titration was stopped immediately colour change was observed (Manokari and Mahipal, 2016; Thirunavukkarasu *et al*, 2016). The stirring continued for 10 mins until a colloid was obtained. The solution consumed 4.9 mL of titrant. The resultant mixture was filtered and cleaned with reagent-grade ethanol and washed with DDW until the pH 7 was gotten. The precipitate was oven-dried at 105 ^oC for 6 hours and calcined in the furnace at 450 ^oC for 3 hours to obtain ZnO-NP. The ZnO-NP obtained was kept in a glass bottle for further characterisation and use.

Green Synthesis of Ag Nanoparticles

5 g of $AgNO_3$ (Thabet *et al*, 2010) powder was measured and synthesised as previously stated in (B) above. The conical flask was rapped with aluminium foil to avoid the photo degradation of silver during titration on the hot plate at 70 ^oC (Njagi *et al*; 2010; Shittu and Ikebana (2017; Vikas et al, 2013) The solution consumed 2.8 mL titrant. The dried Ag-NP obtained was kept in a glass bottle for further characterisation and use.

Production of Nanocomposite Adsorbents

The experimental procedures to produce BKC/Ag, BKC/ZnO, BKC/Ag/ZnO nanocomposites adsorbent for removal of heavy metal contaminants from domestic wastewater are as follows:

Synthesis of BKC/ZnO nanocomposites

1 g of $ZnSO_4.7H_2O$ powder was dissolved in 50 mL of DDW and stirred with magnetic stirrer for 30 min at 150 rpm. 50 mL of the prepared concentration was put in 100 mL conical flask. The conical flask was put on the hot plate and titrated, while continuously stirred at 80 ^oC with *Mangifera Indica* leave extract until the light-yellow colour was formed. The solution consumed 2.6 mL of the titrant. To the suspension formed, 10 g of BKC was dispersed under vigorous stirring for 1 hour at 40 rpm. A homogeneous gel obtained was filtered by Whatman No. 1 filter paper and washed with DDW until the pH 7 was gotten. The gel was oven-dried at 105 ^oC for 6 hours and calcined in the furnace at 450 ^oC for 3 hours to obtain BKC/ZnO nanocomposite adsorbent.

Synthesis of BKC/Ag Nanocomposite

0.5 g of $AgNO_3$ powder was dissolved in 50 mL of DDW and stirred for 30 min at 150 rpm. The prepared concentration was processed as described in (1) above, but stirred at 70 ^oC.

Synthesis of BKC/Ag/ZnO Nanocomposite

0.5 g of $AgNO_3$ and 1 g of $ZnSO_4.7H_2O$ were dissolved in 50 mL of DDW and stirred to get a precursor. The prepared concentration was processed as described in (1) above to obtain BKC/Ag/ZnO nanocomposite adsorbent.

DOI: 10.56892/bima.v7i2.430

Characterisation

The structural changes in the beneficiated kaolin clay, Ag-NP, ZnO-NP, BKC/Ag, BKC/ZnO, BKC/Ag/ZnO nanocomposites adsorbents were analysed using the stated equipment in Table 2 below.

Table 2: Characterisation of Ag/ZnO Nanoparticles, BKC/Ag, BKC/ZnO, BKC/Ag/ZnO Nanocomposites Adsorbents

S/N	Test Equipment and Model	Uses	Parameters	Location
1	X-Ray Diffractometer (XRD), Emma 0141, GCB SCIENTIFIC EQUIPMENT	Determination of mineral phases and compounds in materials. Study of crystal structure of the mineral phases and compounds in materials	Percent of Kaolinite, Quartz and Muscovite in the Beneficiated kaolin clay (BKC) and Nanocomposites (NCs) adsorbents	University of South Africa (UNISA), Johannesburg, South Africa
2	Dispersive X – Ray Fluorescence (XRF) Machine, EDXRF-3600B, OXFORD INSTRUMENT	Chemical analyses of materials	Al_2O_3 and SiO_2 in BKC adsorbents	UNISA, Johannesburg, South Africa
3	HRTEM, TECNAI G2, FEI Netherlands	Determination of Microstructure and particle size of materials	Crystal pattern and Selected Area Electron Diffraction (SAED) of the BKC, NCs, Ag and ZnO nanoparticles	UNISA, Johannesburg, South Africa
4	BET Nitrogen Absorption Analyser, TriStar II 3020, MICROMETRICS, USA	Determination of Pore sizes, Pore Volumes and Surface Areas	Specific surface area, pore size and volume of the BKC, NCs, Ag and ZnO nanoparticles	UNISA, Johannesburg, South Africa
5	UV – Spectrometer, UV – 1800 SHMADZU, Japan	Determination of purity and concentration of a solution	Spectrum peak formation of Ag and ZnO nanoparticles	Centre for Genetic Engineering and Biotechnology, FUT Minna

Wastewater Analyses

Wastewater were analysed to determine COD and BOD concentration. The COD and BOD were analysed by colorimetric and titrimetric methods respectively in line with 21st Edition of American Public Health Association (APHA, 2017) Standard Methods for Examination of Water and Wastewater.

Adsorption Capacity

The adsorption capacity of BKC, BKC/ZnO, BKC/Ag and BKC/Ag/ZnO to remove COD and BOD from the wastewater was tested using both Langmuir isotherms and Freundlich models. The effect of contact time, dosage and temperature were investigated at 10 - 60 mins, 5 – 30 g and 30 – 80 ^{o}C respectively.

Langmuir isotherm

The rate change of concentration due to adsorption equals to the rate of concentration due to desorption as expressed in equation 3.

$$\frac{Ce}{q_e} = \frac{1}{Q_o b} + \frac{Ce}{Qo} \quad (3)$$

Where Ce = Equilibrium concentration (mg/l), q_e = Amount adsorbed at equilibrium time (mg/g), Q_o = Langmuir constants derived from the slope, b = Langmuir constants derived from the intercept, The values of the Langmuir

DOI: 10.56892/bima.v7i2.430

constants were calculated from the intercept and slope of the plot of $\frac{Ce}{q_e}$ versus Ce. The dimensionless separation factor expressed on favourable adsorption nature was calculated from equation 4.

$$\boldsymbol{R_L} = \frac{\mathbf{1}}{(\mathbf{1} + \boldsymbol{bC_i})} \quad (4)$$

Where C_i = Initial concentration of the wastewater (mg/l), b = Langmuir constant (l/mg), R_L= indicate the type of isotherm as shown in Table 3

Table 3: Isotherm Type

R_L Value	Type of Isotherm
$R_L > 1$	Unfavourable
$R_L = 1$	Linear
$R_L < 1$	Favourable
$R_L = 0$	Irreversible

Freundlich isotherm

Freundlich isotherm (Ikhazuangbe et al, 2017) is expressed as shown in equation 5:

$$K_f C_e{}^{\frac{1}{n}} \quad (5)$$

However, the linearized Freundlich adsorption isotherm can be expressed as shown in equation 6.

$$Log\ q_e = Log\ K_f + \frac{1}{n}\ Log\ C_e \quad (6)$$

Where C_e = Equilibrium concentration, q_e = Adsorption capacity at equilibrium stage, K_f and n = Freundlich constants which incorporates all factors affecting the adsorption process (adsorption capacity and intensity). Values of K_f and n were obtained from the intercept and slope of a plot of adsorption capacity (q_e) against equilibrium concentration (C_e). Both parameters K_f and n affect the adsorption isotherm. The larger the K_f and n values, the higher the adsorption capacity (Ikhazuangbe et al, 2017). When the value of n is greater than unity (1< n < 10) that means adsorption process is favourable (Bashir et al, 2013).

Thermodynamic studies

The thermodynamic parameters of the adsorption process were determined from the experimental data obtained at various temperatures using equations 7 - 10 (Bashir et al, 2013; Ikhazuangbe et al, 2017; Al-Kadhi, 2019).

$$\Delta G = -RTlnK_d \quad (7)$$

$$K_d = \frac{q_e}{C_e} \quad (8)$$

$$lnK_d = \frac{\Delta So}{R} - \frac{\Delta Ho}{RT} \quad (9)$$

$$\Delta Go = \Delta Ho - T\Delta So \quad (10)$$

Where Kd = Distribution coefficient for the adsorption, q_e = Amount of contaminants adsorbed on the adsorbent per litre of wastewater at equilibrium, Ce= Equilibrium concentration (mg/L) of the contaminants in wastewater, T = Absolute temperature, R - Gas constant, ΔGo = Gibbs free energy change (kj/mol), ΔHo = Enthalpy change (kj/mol), ΔSo = Entropy change (J/K).

RESULTS AND DISCUSSION

Characterisation Results

XRD analyses

The XRD patterns for raw kaolin clay, BKC, Ag -NP, ZnO-NP, BKC/Ag, BKC/ZnO and BKC/Ag/ZnO were presented in Figures 1 and 2. The broad peaks formation of XRD pattern showed that the raw kaolin clay, beneficiated kaolin, ZnO nanoparticles, BKC/Ag, BKC/ZnO and BKC/Ag/ZnO were polycrystalline while Ag nanoparticles were monocrystalline in nature. The Interplanar spacing and average crystalline sizes obtained as shown in Table 4 ranged from 1.775 nm – 4.712 nm and 26.834 nm - 40.258 nm respectively, at Scherrer's constant of 0.94 and wavelength (λ)of 1.5406 Å. The XRD results confirmed that

DOI: 10.56892/bima.v7i2.430

nanoparticles and nanocomposites adsorbents have been successfully produced in this research work. The indexed peaks are kaolinite while the unindexed peaks are the impurities which are quartz and muscovite as labelled in Figures 1 and 2.

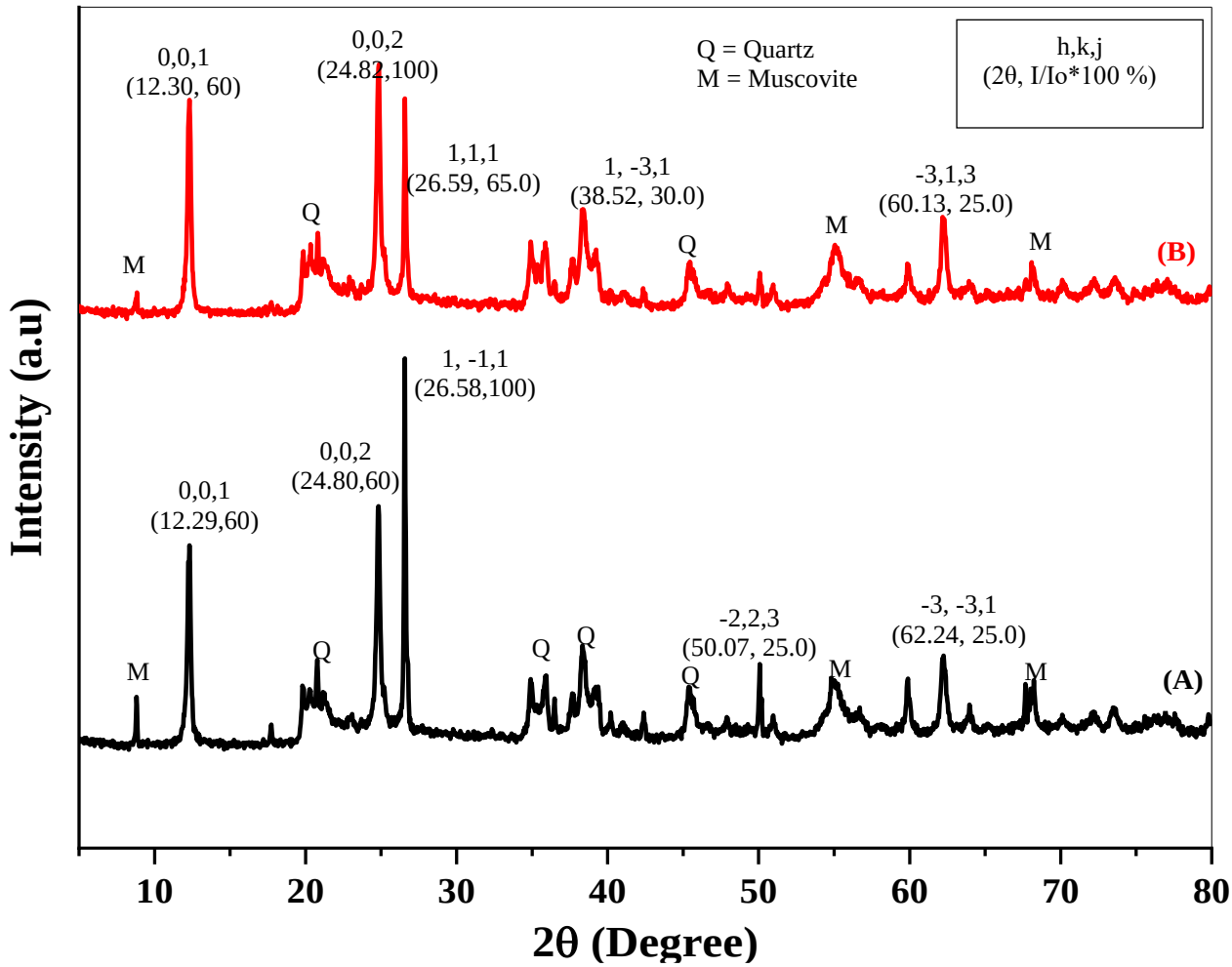

Figure 1: XRD patterns of (A) Raw kaolin and (B) beneficiated kaolin

The data obtained were matched with the database of Joint Committee on Powder Diffraction Standards (JCPDS) file No. 00-004-0783. The JCPDS file revealed the maximum diffraction peaks formation for raw kaolin clay, BKC, BKC/Ag, BKC/ZnO and BKC/Ag/ZnO at 24.82º, 26.58º, 26.60º, 26.63ºand 26.61ºwhich correspond to the crystallographic orientation (h,k,j) of (0,0,2), (1, -1,1), (1,1,1), (1, -1,1) and (1,1,1), respectively at relative intensity of (I/Io*100 %) as shown in Figures 1 and 2.

Bima Journal of Science and Technology, Vol. 7 (2) June, 2023 ISSN: 2536-6041

DOI: 10.56892/bima.v7i2.430

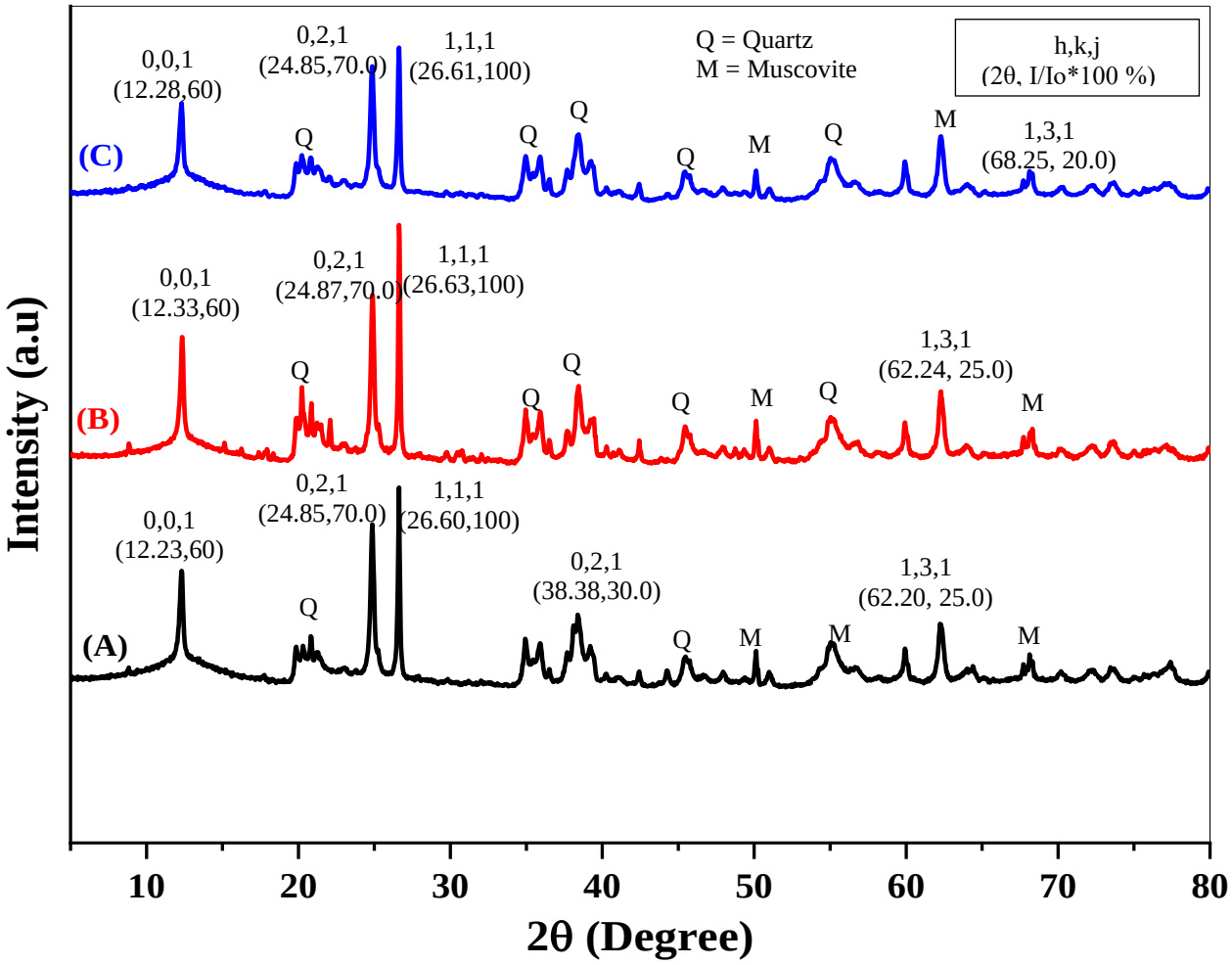

Figure 2: XRD patterns of (A) BKC/Ag (B) BKC/ZnO and (C) BKC/Ag/ZnO

Table 4: Crystallite Size of Ag-NP, ZnO-NP, BKC, BKC/Ag, BKC/ZnO and BKC/Ag/ZnO

Diffraction Angle, 2θ	d- spacing, (nm)	Crystallite Size, D, (nm)
Raw Kaolin	3.499	40.258
BKC	3.532	28.114
Ag Nanoparticles	1.775	30.629
ZnO Nanoparticles	3.435	32.038
BKC/Ag	3.818	25.574
BKC/ZnO	4.712	35.692
BKC/Ag/ZnO	3.887	26.934

XRF analyses

The XRF analysis was further carried out on the obtained Ag-NP, ZnO-NP, BKC, BKC/Ag, BKC/ZnO and BKC/Ag/ZnO as shown in Table 5. The SiO_2/Al_2O_3 ratios of BKC/Ag, BKC/ZnO and BKC/Ag/ZnO nanocomposites adsorbents ware 1.5170, 1.4818 and 1.5231 respectively. The SiO_2/Al_2O_3 ratio, a function of the mineral

DOI: 10.56892/bima.v7i2.430

phase present in BKC/Ag, BKC/ZnO and BKC/Ag/ZnO nanocomposites, indicated that a purer kaolinite has been produced when compared with the raw kaolin clay ratio of 1.54. The closer the SiO_2/Al_2O_3 ratio to unity the purer the kaolin. Loss on ignition (LOI) for BKC/Ag, BKC/ZnO and BKC/Ag/ZnO nanocomposites adsorbents was found to be 9.61%, 16.31% and 12.37 % respectively.

Table 5: Mineralogy composition of Ag-NP, ZnO-NP, BKC, BKC/Ag, BKC/ZnO and BKC/Ag/ZnO

Compound	Raw Kaolin Clay (%)	Beneficiated Kaolin Clay	ZnO Nanoparticles	Ag Nanoparticles	BKC/Ag	BKC/ZnO	BKC/Ag/ZnO
Fe_2O_3 %	1.23	1.24	0.01	0.00	1.00	1.04	0.97
MnO %	0.00	0.00	0.00	0.00	0.00	0.01	0.00
Cr_2O_3 %	0.02	0.02	0.01	0.00	0.03	0.03	0.02
V_2O_5 %	0.00	0.00	0.00	0.00	0.03	0.03	0.02
TiO_2 %	1.69	1.75	0.05	0.01	1.61	1.69	1.58
CaO %	0.33	0.02	0.18	0.02	0.00	0.09	0.05
K_2O %	0.61	0.63	0.42	0.01	0.56	0.53	0.54
P_2O_5 %	0.07	0.05	0.04	0.00	0.05	0.04	0.03
SiO_2 %	52.64	48.55	0.00	0.00	45.80	44.13	46.21
Al_2O_3 %	34.18	35.95	0.02	0.00	30.19	29.78	30.34
MgO %	0.23	0.03	0.06	0.00	0.00	0.00	0.00
Na_2O %	0.11	0.14	9.21	0.02	0.18	1.16	0.40
LOI %	8.90	11.62	52.13	51.10	9.61	16.31	12.37
Total	100	100	62.15	53.56	89.10	94.82	92.55
SiO_2/Al_2O_3 Ratio	1.54	1.35	**0.000**	**0.000**	**1.517**	**1.4818**	**1.5231**

HRTEM Analysis

The crystal patterns of the raw kaolin clay are presented in Plates I (a – b). The crystallinity of the kaolin clay was examined using Selected Area Electron Diffraction (SAED) pattern as shown in Plates I (c). The bright spots and rings of the SAED pattern suggested that the raw kaolin clay, is polycrystalline in nature.

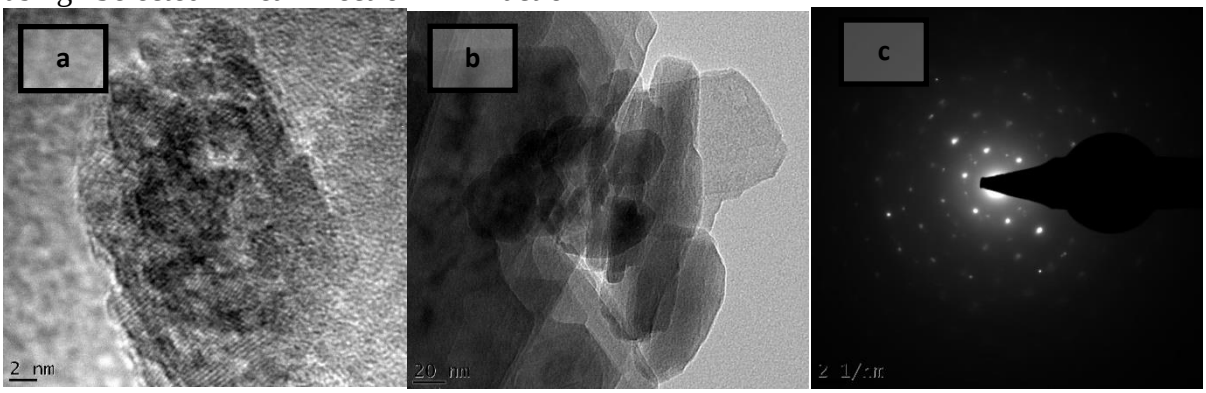

Plate I: HRTEM (a – b) and SAED (c) Images of Raw Kaolin Clay

DOI: 10.56892/bima.v7i2.430

HRTEM images in Plate II (a – b) showed the structure of the BKC with kaolinite particles of varying sizes arranged in face-to-face patterns. The crystal structure in Plate II (c) showed bright rings of SAED patterns which are polycrystalline, with each ring depicted diffraction pattern of BKC particles.

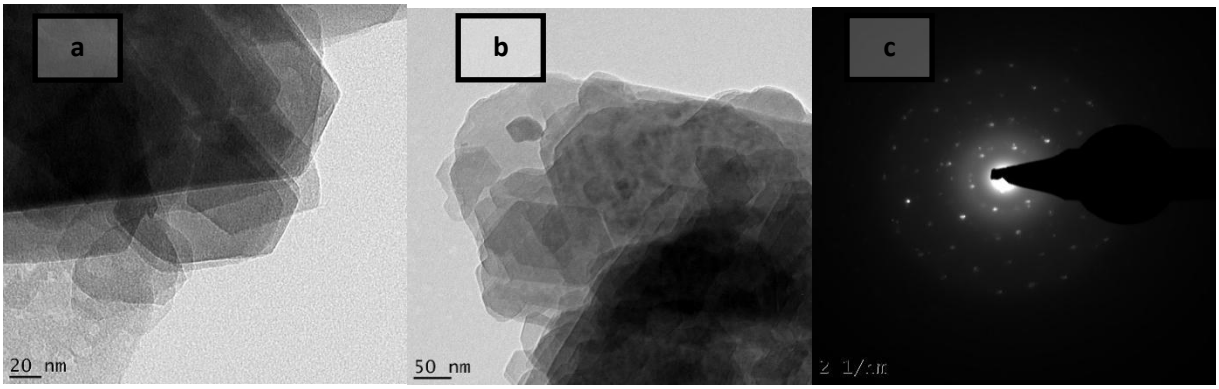

Plate II:HRTEM (a – b) and SAED (c) Images of Beneficiated Kaolin Clay Adsorbent

The crystallinity of Ag-NP was examined using SAED pattern and the results are presented in Plate III (a - c). The bright spots and rings of the SAED patterns suggested the Ag-NP is monocrystalline in nature. SAED resolution pattern are consistent with the XRD and XRF results of Ag-NP as earlier stated in this study.

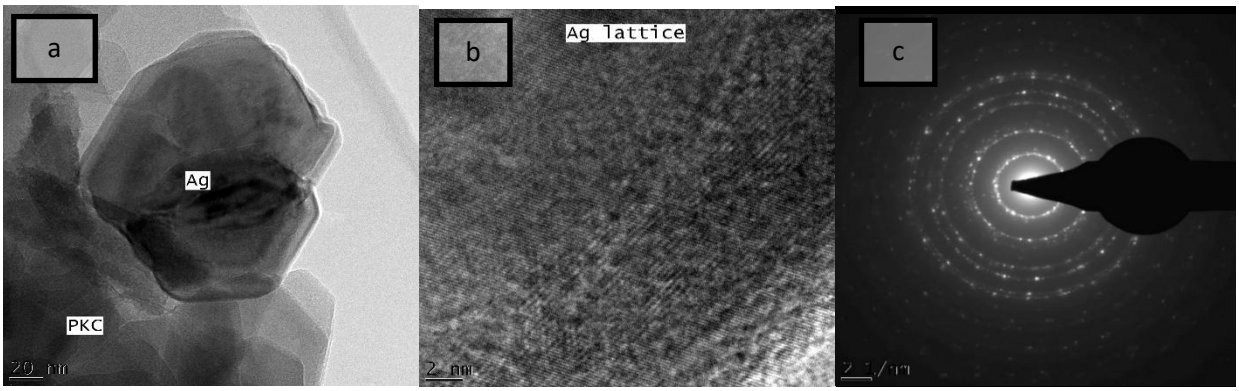

Plate III: HRTEM (a – b) and SAED (c) Images of BKC/Ag Nanocomposite Adsorbents

The crystal structure of ZnO-NP was analysed by HRTEM to know the crystal pattern at the scales approaching a single atom as presented in Plate IV (a – b). The SAED pattern in Plate IV (c) showed faded circles which suggested that the ZnO-NP is polycrystalline in nature.

DOI: 10.56892/bima.v7i2.430

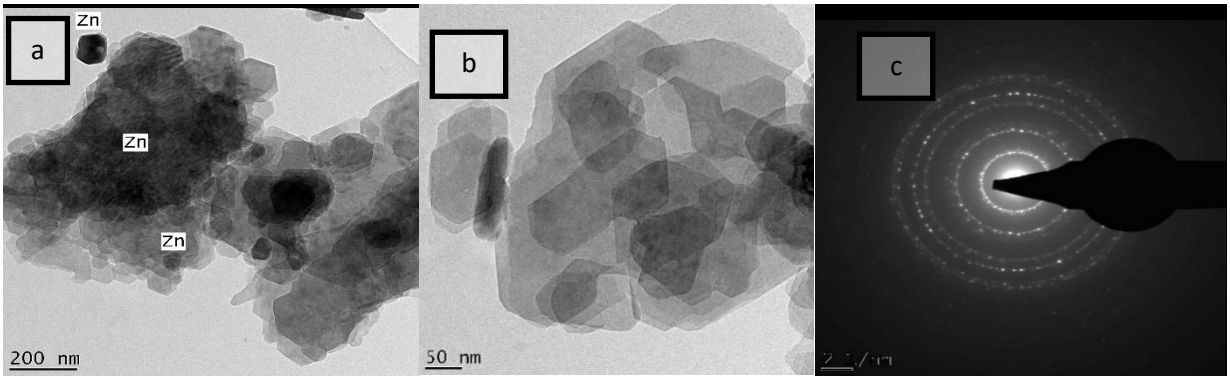

Plate IV: HRTEM (a – b) and SAED (c) Images of BKC/ZnO Nanocomposite Adsorbents

The heavy dark colour images in V (a - b) indicated the presence of silver atoms and impregnation of Ag-NP on BKC, while the grey colour indicated crystal of different sizes. The bright spots and rings of the SAED pattern in Plate V (c) suggested that the BKC/Ag nanocomposite adsorbentis polycrystalline. The HRTEM images and SAED resolution pattern obtained were consistent with the results of XRD and XRF characterization in this study.

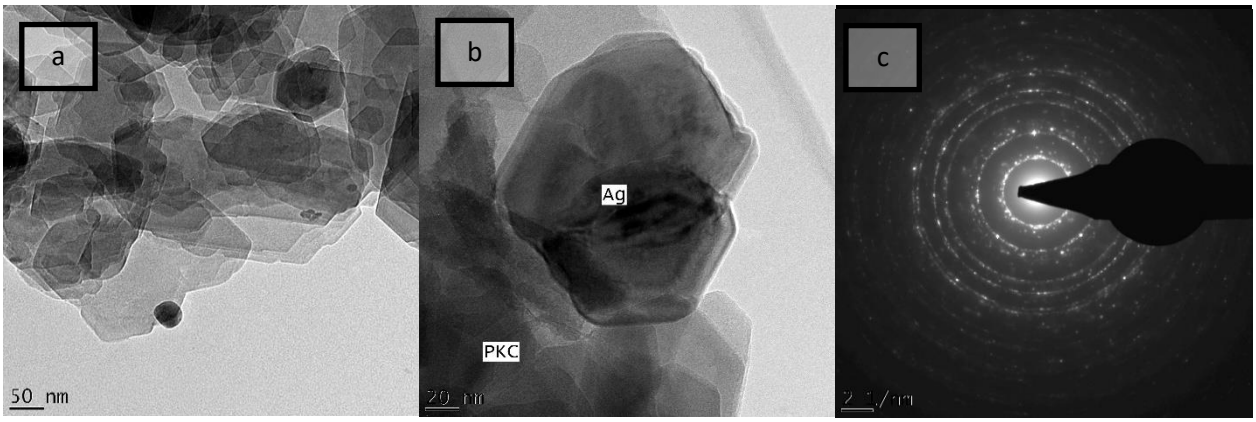

Plate V: HRTEM (a – b) and SAED (c) Images of BKC/Ag/ZnO Nanocomposite Adsorbents

The heavy dark colour images in VI (a - b) indicated the presence of zinc atoms and impregnation of ZnO-NP on BKC as previously described in plate V. The bright spots and rings of the SAED pattern suggested that the nanocomposite adsorbent produced is polycrystalline in nature.

DOI: 10.56892/bima.v7i2.430

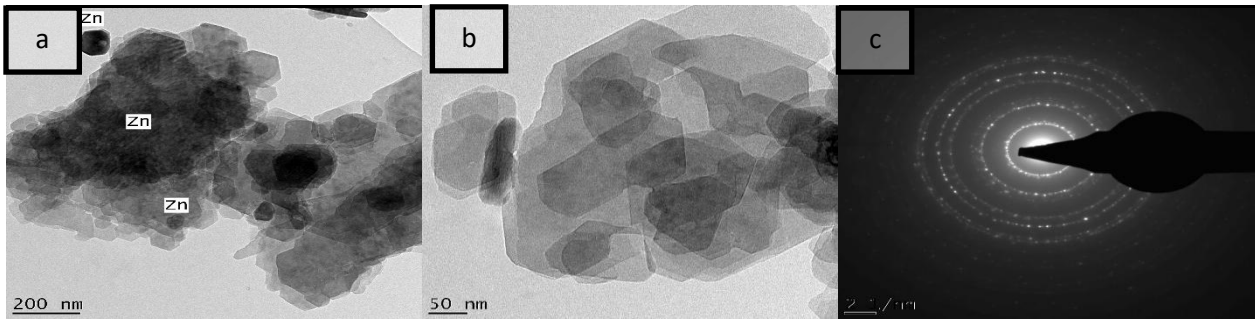

Plate VI: *HRTEM (a – b) and SAED (c) Images of BKC/ZnO Nanocomposite Adsorbents*

HRTEM images in Plate VII (a – b) clearly showed the impregnation of Ag-np and ZnO-np on BKC.The heavy dark colour images in Plate VII (c) indicated the presence of zinc and silver atoms, while the light or grey colour indicated crystal of different sizes. The HRTEM images and SAED resolution pattern obtained were consistent with the earlier results of XRD and XRF characterisation.

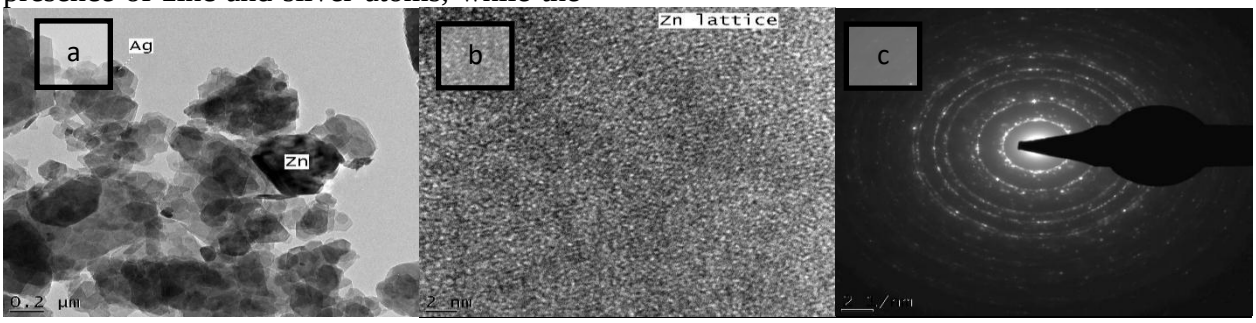

Plate VII:*HRTEM (a – e) and SAED (f) Images of BKC/Ag/ZnO Nanocomposite Adsorbent*

BET analyses

Nitrogen (N_2) adsorption-desorption isotherm of the BKC, BKC/Ag, BKC/ZnO and BKC/Ag/ZnO nanocomposites adsorbents are displayed in Figures 3, 4, 5 and 6. The nanocomposite adsorbents produced belongs to type IV isotherm with a hysteresis loop, which resulted from capillary condensation in the mesopores (diameter, $2 < d < 50$ nm) at the relative pressure range of 0.45 –0.9, P/Po.

The quasi-overlapping adsorption-desorption curves of the produced nanocomposite adsorbents indicated that the N_2 adsorption-desorption isotherm curve of the adsorbents are classified as Type IV, indicating a purely mesoporous material with small pore size.The adsorption isotherms of BKC, BKC/Ag, BKC/ZnO and BKC/Ag/ZnO rose progressively during the relative pressure range of 0 – 0.4 P/Po (Figures 3 – 6), which means mono-molecule layer adsorption occurring on the surface.

Bima Journal of Science and Technology, Vol. 7 (2) June, 2023 ISSN: 2536-6041

DOI: 10.56892/bima.v7i2.430

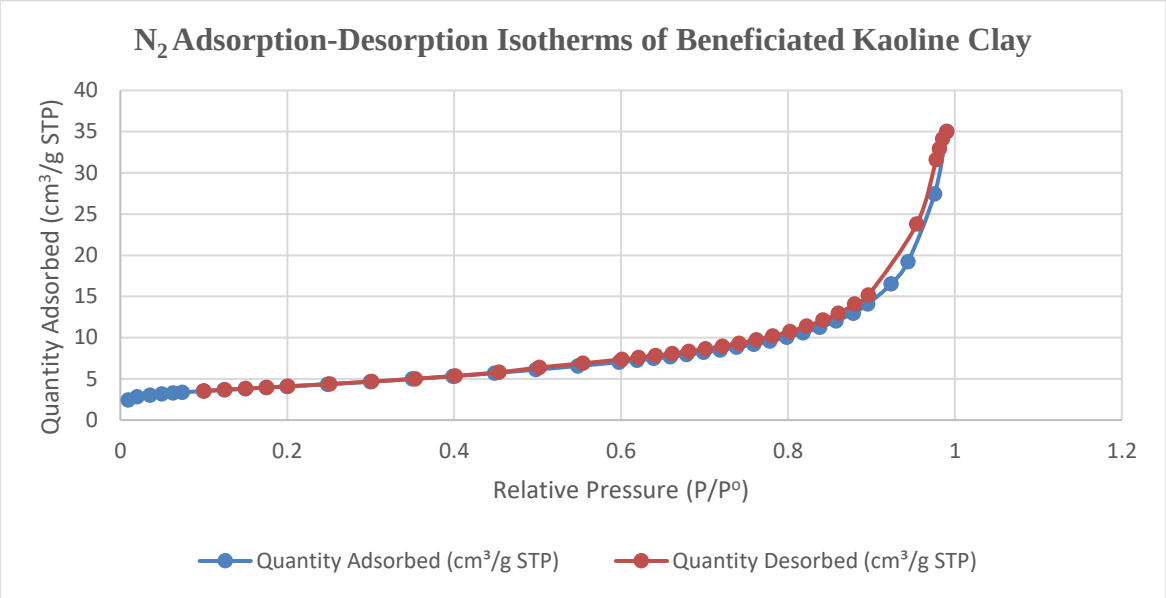

Figure 3: N_2 Adsorption-Desorption Isotherms of Beneficiated Kaolin

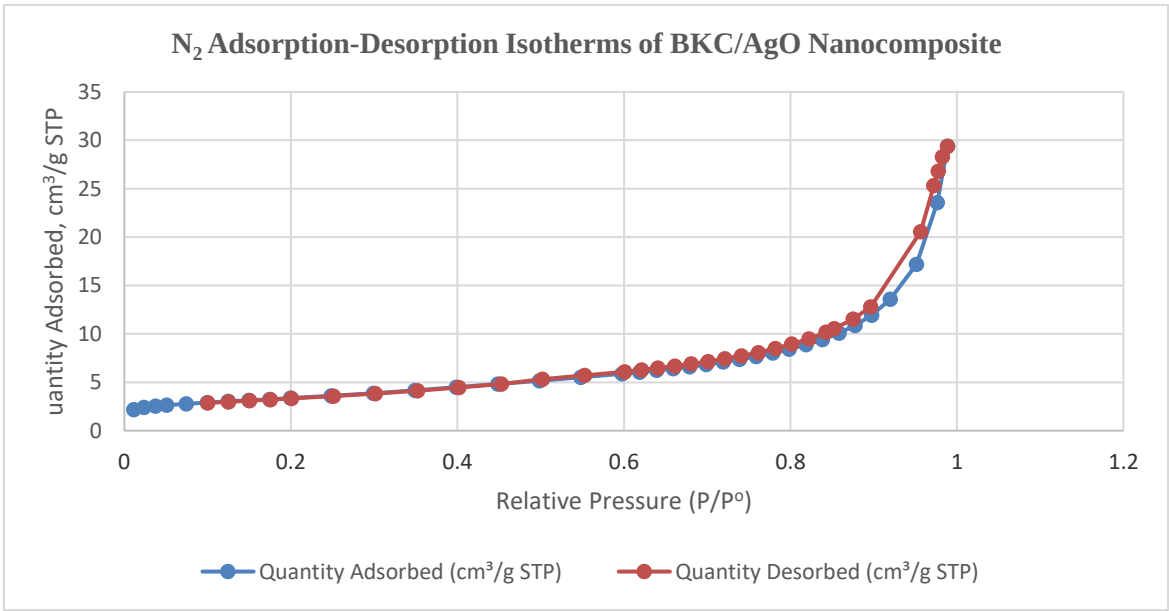

Figure 4:N_2 Adsorption-Desorption Isotherms of BKC/Ag Nanocomposite

Bima Journal of Science and Technology, Vol. 7 (2) June, 2023 ISSN: 2536-6041

DOI: 10.56892/bima.v7i2.430

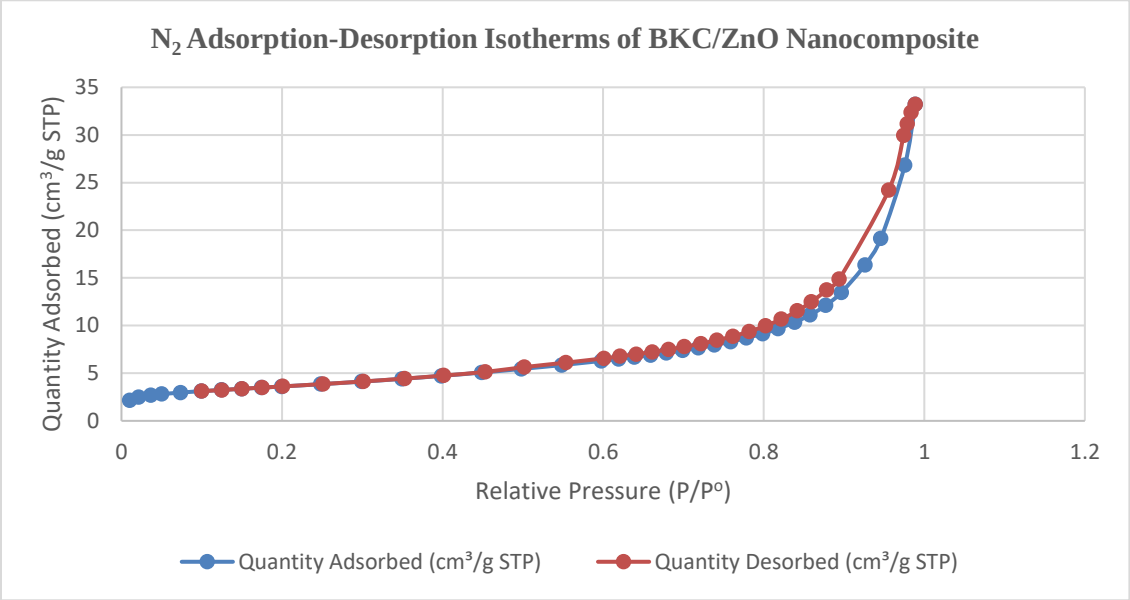

Figure 5: N_2 Adsorption-Desorption Isotherms of BKC/ZnO Nanocomposite

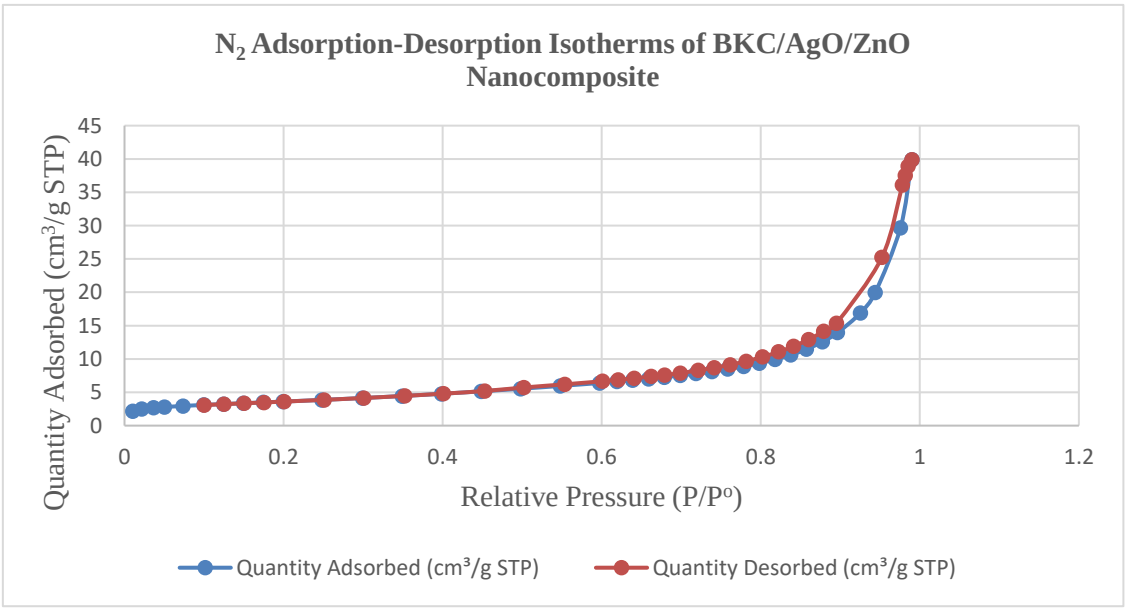

Figure 6: N_2 Adsorption-Desorption Isotherms of BKC/Ag/ZnO Nanocomposite

The adsorption curves rose steadily, resulting in the saturation of mono-molecule layer adsorption followed by the multi-molecular layer adsorption. When the relative pressure was 0.4 – 0.9 P/Po, the desorption branch was obviously higher than the adsorption branch, along with the appearance of capillary condensation, which resulted in the hysteresis loop. At the relative pressure of 0.4 – 0.9 P/Po, the adsorption branch and desorption branch suddenly rose and coincided at the end.

Also, the occurrences of hysteresis loops indicated that the BKC, BKC/Ag, BKC/ZnO and BKC/Ag/ZnO had a lot of mesopores. Similarly, the smaller adsorption amount at

DOI: 10.56892/bima.v7i2.430

P/Po < 0.4 and the large adsorption amount at P/Po > 0.9 showed that the BKC/Ag, BKC/ZnO and BKC/Ag/ZnO had a certain number of macropores (d > 50 nm) and a small amount of micropores (d < 2 nm). This particular characteristic is ascribed mainly to mesoporous structures. Furthermore, hysteresis loops of the BKC, BKC/Ag, BKC/ZnO and BKC/Ag/ZnO belong to type H3, demonstrating that wedge-shaped pores took the primary position in the nanocomposite adsorbents. The BET analysis results showed the BKC, BKC/Ag, BKC/ZnO and BKC/Ag/ZnO as promosing materials to be used as adsorbent for filter production.

Domestic Wastewater Analyses

Domestic wastewater collected was analysed to determine the concentration of COD and BOD in the initial wastewater before treatment using BKC, BKC/Ag, BKC/ZnO and BKC/Ag/ZnO nanocomposite adsorbents. The obtained analytical results for BOD and COD, in the domestic wastewater collected, were 30.6 mg/L and 312 mg/L respectively. These results were found to be far above the maximum permissible limit of 4 mg/L and 30 mg/L set for BOD and COD by NESREA, 2011, and therefore treatments were required.

Adsorption Studies

Effect of contact time

The effect of contact time on the adsorption of COD and BOD onto BKC, BKC/ZnO, BKC/Ag and BKC/Ag/ZnO nanocomposites adsorbents was studied at contact time of 10, 20, 30, 40, 50 and 60 mins using an adsorbent dosage of 25 g/100 mL of wastewater at a temperature of 29.5 ^{o}C and pH of 6.9. It was observed that a reduction in the fraction of COD and BOD occurred with corresponding increase in the contact time for the produced nanocomposite adsorbents as presented in Table 6. Rapid adsorption rates were obtained between the contact time of 10 – 40 mins. On reaching the equilibrium adsorption, the rate of adsorption equals the rate of desorption; therefore, the slow uptake and the slight or no decrease in COD and BOD concentration removal with further increase in contact time might be due to saturation of the surface area of the adsorbent with pollutants.

Table 6: Effect of Contact Time

Adsorbents	**Wastewater (mg/L)**	***Effect of contact time on COD concentration (mg/L)***					
		10 Mins	**20 Mins**	**30 Mins**	**40 Mins**	**50 Mins**	**60 Mins**
BKC	312	37.2	26.04	23.436	23.202	22.738	22.738
BKC/ZnO	312	37.1	25.97	23.373	23.139	22.676	22.676
BKC/Ag	312	36.9	25.83	23.247	23.015	22.554	22.554
BKC/Ag/ZnO	312	34.2	23.94	21.546	21.331	20.904	20.904
		Effect of contact time on BOD concentration (mg/L)					
BKC	30.6	5.23	3.661	3.2949	3.262	3.197	3.197
BKC/ZnO	30.6	8.49	5.943	5.3487	5.295	5.189	5.189
BKC/Ag	30.6	8.48	5.936	5.3424	5.289	5.183	5.183
BKC/Ag/ZnO	30.6	8.25	5.775	5.1975	5.146	5.043	5.043

DOI: 10.56892/bima.v7i2.430

Effect of dosage

The effects of adsorbent dosage when treated with BKC, BKC/ZnO, BKC/Ag and BKC/Ag/ZnO nanocomposites adsorbents to remove the COD and BOD concentration from wastewater was studied at adsorbent dosages of 5 – 30 g, constant pH of 6.9, temperature of 29.4 ^{o}C and contact time fixed at 30 mins. The higher the adsorbent dosages used in the treatment, the higher the COD and BOD concentration removal efficiencies from the wastewater. The observed trend in terms of COD and BOD removal were BKC/Ag/ZnO > BKC/Ag > BKC/ZnO > BKC as shown in Table 7. This is because of an increase in the availability of the active binding exchangeable sites and large surface areas of the adsorbents (Abukhadra and Mohamed, 2019).

Table 7: Effect of Dosage

Adsorbents	**Wastewater (mg/L)**	**Effect of contact dosage on COD concentration (mg/L)**					
		5 g	**10 g**	**15 g**	**20 g**	**25 g**	**30 g**
BKC	312	144	101	90.7	89.8	88.0	88.0
BKC/ZnO	312	138	96.6	86.9	86.1	84.3	84.3
BKC/Ag	312	139	97.3	87.6	86.7	85.0	85.0
BKC/Ag/ZnO	312	130	91.0	81.9	81.1	79.5	79.5
		Effect of contact dosage on BOD concentration (mg/L)					
BKC	30.6	15.2	10.64	9.576	9.480	9.291	9.291
BKC/ZnO	30.6	14.3	10.01	9.009	8.919	8.741	8.741
BKC/Ag	30.6	13.7	9.59	8.631	8.545	8.374	8.374
BKC/Ag/ZnO	30.6	12.9	9.03	8.127	8.046	7.885	7.885

Effect of temperatures

The effect of temperatures on the adsorption of COD and BOD concentration onto BKC, BKC/ZnO, BKC/Ag and BKC/Ag/ZnO nanocomposites adsorbents was studied at temperature of 30, 40, 50, 60, 70 and 80 ^{o}C using an adsorbent dosage of 25 g/100 ml of wastewater at a temperature of 29.5 ^{o}C and pH of 6.9. The increase in temperature from 30 ^{o}C- 80 ^{o}C for the nanocomposite adsorbents gradually increased heavy metal adsorption. Slow uptake of pollutants was observed from 70 - 80 ^{o}C for nanocomposite adsorbent as presented in Table 8. The slow uptake and the slight or no increase in concentration removal with further increase in temperature might be due to saturation of the surface area of the adsorbent with pollutants.

DOI: 10.56892/bima.v7i2.430

Table 8: Effect of Temperature

Adsorbents	Wastewater (mg/L)	Effect of contact temperature on COD concentration (mg/L)					
		30°C	40°C	50°C	60°C	70°C	80°C
BKC	312	37.2	26.0	22.1	19.9	16.7	16.5
BKC/ZnO	312	37.1	26.0	22.1	19.9	16.7	16.5
BKC/Ag	312	36.9	25.8	22.0	19.8	16.6	16.4
BKC/Ag/ZnO	312	34.2	23.9	20.3	18.3	15.4	15.2
		Effect of contact temperature on BOD concentration (mg/L)					
BKC	30.6	5.23	3.661	3.1119	2.801	2.353	2.325
BKC/ZnO	30.6	8.49	5.943	5.0516	4.546	3.819	3.774
BKC/Ag	30.6	8.48	5.936	5.0456	4.541	3.814	3.769
BKC/Ag/ZnO	30.6	8.25	5.775	4.9088	4.418	3.711	3.667

Adsorption Isotherm

Langmuir isotherms

Tables 9 showed the Langmuir model isotherm for the determination of $Q_o$and b**.** From the slopes and intercepts of the plots of $\frac{Ce}{q_e}$ versus Ce for the removal of COD and BOD in wastewater, the model showed the multilayer adsorption patterns and the fitting to the heterosporous nature of BKC, BKC/ZnO, BKC/Ag and BKC/Ag/ZnO nanocomposite adsorbents. It was evident that the linear correlation coefficients (R^2) for BKC, BKC/ZnO, BKC/Ag and BKC/Ag/ZnO nanocomposite adsorbents in the removal of COD and BOD were all greater than 0.90. This showed that the experimental data moderately fit Langmuir adsorption isotherm. The calculated R_L values for COD and BOD gave an indication of the favourability of the adsorption process and type of the isotherm which is R_L< 1.The results show that BKC, BKC/Ag, BKC/ZnO and BKC/Ag/ZnO nano composite adsorbents corresponded to the Langmuir model.

Table 9: Langmuir Adsorption Isotherm Constants for BKC, BKC/Ag, BKC/ZnO and BKC/Ag/ZnO

Parameters	Sample	Intercept = 1/Qob	Slope = 1/Qo	Qo	b	R_L	R^2
COD	BKC	0.1441	0.0014	714.2857	0.009715	0.248063	0.9842
	BKC/Ag	0.1437	0.0013	769.2308	0.009047	0.261606	0.9951
	BKC/ZnO	0.1511	0.0013	769.2308	0.008604	0.271421	0.9904
	BKC/Ag/ZnO	0.1423	0.0013	769.2308	0.009136	0.259719	0.9917
BOD	BKC	0.1020	0.0085	117.6471	0.083333	0.28169	0.9524
	BKC/Ag	0.1007	0.0075	133.3333	0.074479	0.304967	0.9735
	BKC/ZnO	0.0914	0.0078	128.2051	0.085339	0.276903	0.9782
	BKC/Ag/ZnO	0.0661	0.0087	114.9425	0.131619	0.198905	0.9784

Bima Journal of Science and Technology, Vol. 7 (2) June, 2023 ISSN: 2536-6041

DOI: 10.56892/bima.v7i2.430

The Langmuir plots of $\frac{Ce}{q_e}$ versus Ce for the removal of COD and BOD exhibited linearity and good correlation coefficient as presented in Figure 7 (a – h).

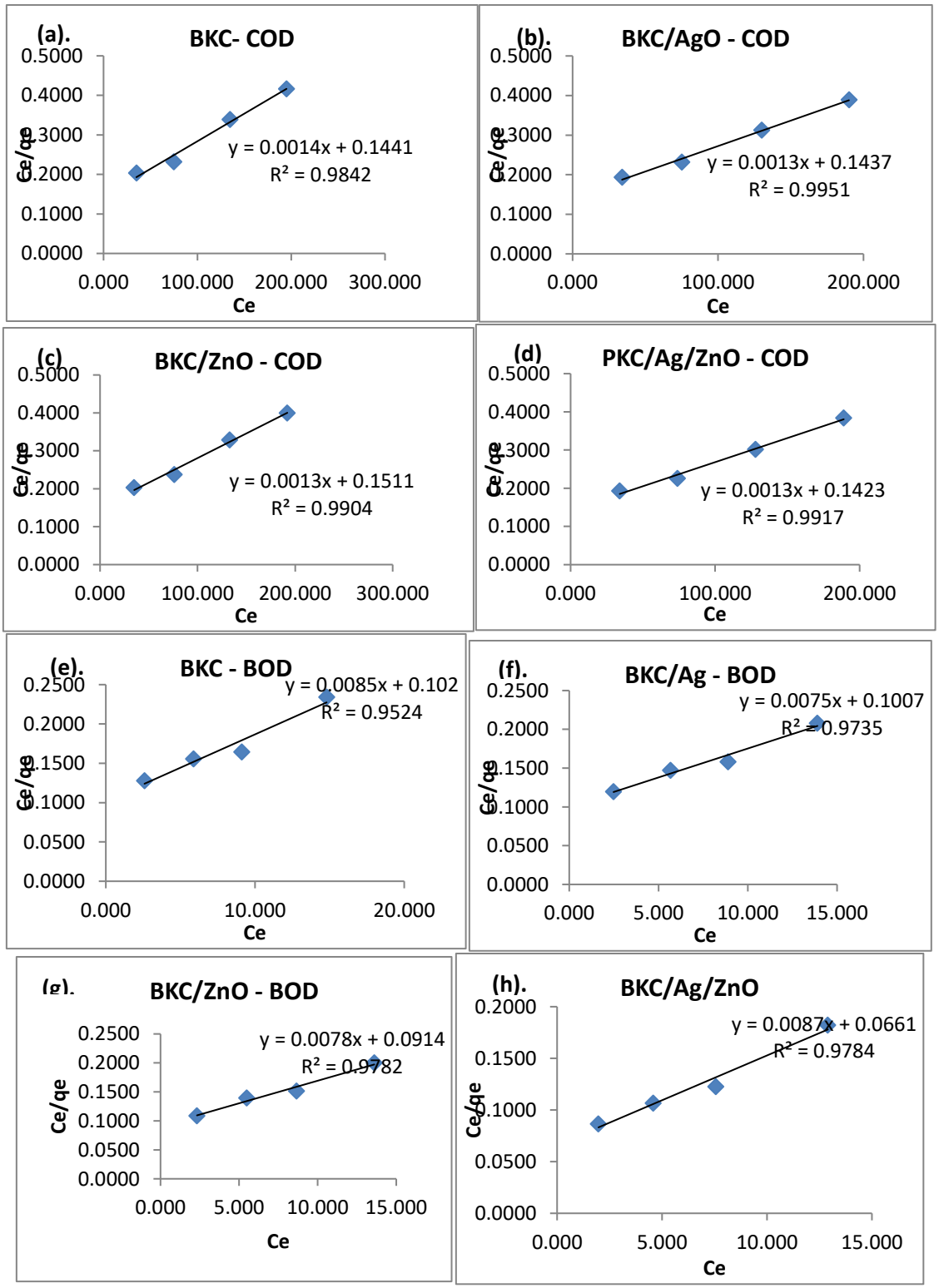

Figure 7 (a – h): Langmuir Adsorption Isotherm for COD and BOD Removal

DOI: 10.56892/bima.v7i2.430

Freundlich adsorption isotherm

Table 10 showed the Freundlich model isotherm values of K_f and n obtained from the intercept and slope of a plot of adsorption capacity (q_e) against equilibrium concentration (C_e). Both parameters K_f and n affect the adsorption isotherm. The larger the $K_f$and n values, the higher the adsorption capacity. From the plot of adsorption capacity (q_e) against equilibrium concentration (C_e) for the removal of COD and BOD in wastewater, the model showed the multilayer adsorption patterns and the fitting to the heterosporous nature of BKC, BKC/Ag, BKC/ZnO and BKC/Ag/ZnO nano composite adsorbents. It was evident that the linear correlation coefficients (R^2) for BKC, BKC/ZnO, BKC/Ag and BKC/Ag/ZnO nanocomposite adsorbents in the removal of COD and BOD were greater than 0.90. This showed that the experimental data moderately fit Freundlich adsorption isotherm. The larger the $K_f$and n values, the higher the adsorption capacity. Furthermore, the magnitude of the exponent n gave an indication of the favourability of the adsorption process. When the value of n is greater than unity (1< n < 10), the adsorption process is favourable. The calculated n values for COD and BOD gave an indication of the favourability of the adsorption process as shown in the Table 10. The values of R^2 were very close to unity, showing a strong agreement with the Freundlich isotherm.

Table 10: Freundlich Adsorption Isotherm Constants for BKC, BKC/Ag, BKC/ZnO and BKC/Ag/ZnO

Parameter	Sample	Intercept = log K	Slope = 1/n	n	K	R^2
COD	BKC	1.3812	0.5729	1.745505	24.0547	0.9588
	BKC/Ag	1.3598	0.5929	1.686625	22.89813	0.9775
	BKC/ZnO	1.3367	0.5978	1.672800	21.71201	0.9741
	BKC/Ag/ZnO	1.3495	0.6015	1.662510	22.36145	0.9723
BOD	BKC	1.0437	0.6800	1.470588	11.05860	0.9718
	BKC/Ag	1.0508	0.7013	1.425923	11.24087	0.9866
	BKC/ZnO	1.0915	0.6762	1.478852	12.34525	0.9879
	BKC/Ag/ZnO	1.1970	0.6249	1.600256	15.73983	0.9680

The Freundlich adsorption plot of isotherm values of K_f and n obtained from the intercept and slope of a plot of adsorption capacity (q_e) against equilibrium concentration (C_e). exhibited linearity and good correlation coefficient as shown in Figure 8 (a – h).

Bima Journal of Science and Technology, Vol. 7 (2) June, 2023 ISSN: 2536-6041

DOI: 10.56892/bima.v7i2.430

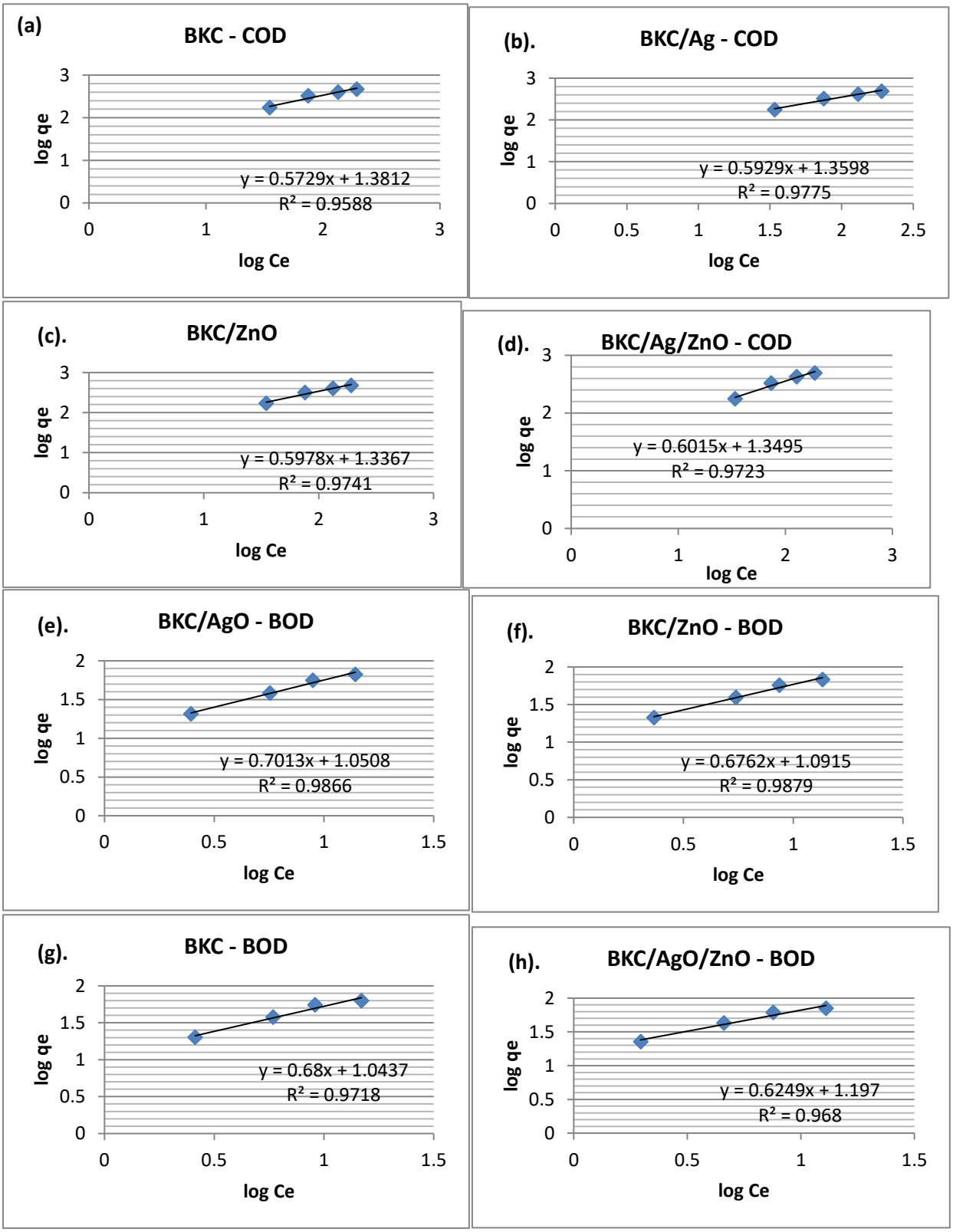

Figure 8 (a – h): Freundlich Adsorption Isotherm for COD and BOD Removal

Bima Journal of Science and Technology, Vol. 7 (2) June, 2023 ISSN: 2536-6041

DOI: 10.56892/bima.v7i2.430

Table 11: Thermodynamic Parameters of COD and BOD using BKC, BKC/Ag, BKC/ZnO and BKC/Ag/ZnO

Parameters	Adsorbents	Intercept = $\Delta S^o/R$	Slope = $-\Delta H^o/R$	R^2	R ($Jmol^{-1} K^{-1}$)	ΔS^o	ΔH^o	ΔG^o					
								303	313	323	333	343	353
COD	**BKC**	9.5828	-1841.2	0.9307	8.3145	79.67619	15308.66	-8833.23	-9629.99	-10426.8	-11223.5	-12020.3	-12817
	BKC/ZnO	9.5844	-1840.8	0.9308	9.3145	89.27389	17146.13	-9903.86	-10796.6	-11689.3	-12582.1	-13474.8	-14367.6
	BKC/Ag	9.5877	-1839.9	0.9308	10.3145	98.89233	18977.65	-10986.7	-11975.7	-12964.6	-13953.5	-14942.4	-15931.3
	BKC/Ag/ZnO	9.6347	-1828.5	0.9312	11.3145	109.0118	20688.56	-12342	-13432.1	-14522.3	-15612.4	-16702.5	-17792.6
BOD	**BKC**	9.4053	-1912.6	0.9284	8.3145	78.20037	15902.31	-7792.4	-8574.4	-9356.41	-10138.4	-10920.4	-11702.4
	BKC/ZnO	9.3551	-2080.3	0.9226	9.3145	87.13808	19376.95	-7025.88	-7897.26	-8768.65	-9640.03	-10511.4	-11382.8
	BKC/Ag	9.3548	-2079.7	0.9226	10.3145	96.49008	21451.07	-7785.43	-8750.33	-9715.23	-10680.1	-11645	-12609.9
	BKC/Ag/ZnO	9.3488	-2066.8	0.9231	11.3145	105.777	23384.81	-8665.62	-9723.39	-10781.2	-11838.9	-12896.7	-13954.5

DOI: 10.56892/bima.v7i2.430

Enthalpy (ΔH), Gibb's Free Energy (ΔG) and Entropy (ΔS) of Adsorption

The values of enthalpy change (ΔH^o) and entropy change (ΔS^o) were obtained from the slope and intercept of ln K_d versus 1/T plots. The values of $\Delta H^o$and ΔS^owere found to be positive for COD and BOD as presented in Table 11. The positive values of ΔH^oshowed that the adsorption processes of the nanocomposite adsorbents were endothermic in nature. The negative values of ΔG^oindicated the adsorption of COD and BOD onto the nanocomposite adsorbents, is spontaneous and exothermic over the study range of temperatures (Abbas *et al.*, 2020).

CONCLUSION

Nanocomposite adsorbents were successfully produced and characterised. The efficacy of the adsorbents produced in the removal of COD and BOD concentration from domestic wastewater followed this trend: BKC/Ag/ZnO > BKC/Ag > BKC/ZnO > BKC. Both the Langmuir and Freundlich isotherms models were favourable, thus provided the good fits for predicting the adsorption of COD and BOD. ΔH^o and ΔS^o were positive which showed that the adsorptions processes were endothermic in nature. The nanocomposite adsorbents produced is therefore recommended for use in the treatment of domestic wastewater.

REFERENCES

Abdullah, A. A., Mansor B.A., Naif M.A., Halimah M.K., Hussein M.Z. & Nor A.I. (2017). Preparation of Zeolite/Zinc Oxide Nanocomposites for toxic metals removal from water. *Elsevier Results in Physics* 7 (2017). http://dx.doi.org/10.1016/j.rinp.2017.01.036, pp723–731

Adewole, T.A. (2006). Changing the face of my local community through waste to wealth programme in Lagos State, Nigeria. *Strength Based Strategies 2006*, Close 12 House 10 Satellite Town, Lagos, pp 8 – 11.

Al-Kadhi, N. S. (2019). The kinetic and thermodynamic study of the adsorption Lissamine Green B dye by micro-particle of wild plants from aqueous solutions. *The Egyptian Journal of Aquatic Research*.

Anijiofor, S.C., Azreen M.J., Jabbar S., Saad S., & Chandima G. (2017). Aerobic and Anaerobic Sewage Biodegradable Processes: The Gap Analysis, *International Journal of Research in Environmental Science*Volume 3, Issue 3 2017, ISSN No. (Online) 2454-9444.

APHA (2017). *Standard methods for Examination of Water and Wastewater*. APHA, AWWA, WEF. 23rd Edition, Published by E and FN SPON, Washington D.C

Aroke, U. O. & Onatola-Morakinyo S. (2016). Comparative Sorption of Diatomic Oxyanions onto HDTMA-Br Modified Kaolinite Clay. *International Journal of Engineering and Science* Vol.6, Issue 7 (August 2016), ISSN (e): 2278-4721, ISSN (p):2319-6483, www.researchinventy.com, pp 01-09.

Auta, M. & Hameed B.H. (2013). Acid modified local clay beads as effective low-cost adsorbent for dynamic adsorption of methylene blue. *Journal of Industrial and Engineering Chemistry.*

Bachiri, E.M., Akichouh E., Miz H., Salhi S. & Tahani A. (2014). Adsorptions desorption and kinetics studies of Methylene Blue Dye on Na-bentonite from Aqueous Solution. *IOSR Journal of Applied Chemistry* (IOSR-JAC) e-ISSN: 2278-5736.Volume 7, Issue 7 Ver. III. (July. 2014), www.iosrjournals.org, pp 60-78.

Bachiri, E.M., Akichouh E., Miz H., Salhi S. & Tahani A. (2014). Adsorptions desorption and kinetics studies of Methylene Blue Dye on Na-bentonite from Aqueous Solution. *IOSR Journal of Applied Chemistry* (IOSR-JAC) e-ISSN: 2278-5736.Volume 7, Issue 7 Ver. III. (July. 2014), www.iosrjournals.org, pp 60-78.

Benakashani, F., Allafchian, A.R., & Jalali. S.A.H. (2016). Biosynthesis of silver nanoparticles using Capparis spinosa L. leaf extract and their antibacterial activity. Elsevier published Karbala *International Journal of Modern Science*..

Chan, Y. J., Chong, M. F., Law, C. L., & Hassell, D. G. (2009). A review on anaerobic–aerobic treatment of industrial and municipal wastewater. School of Chemical and Environmental Engineering, Faculty of Engineering, The University of Nottingham1385-8947/$ – see front matter © 2009 *Elsevier B.V.*

Cheng, Q, Li H, Xu Y, Chen S, Liao Y, & Deng F. (2017) Study on the adsorption of nitrogen and phosphorus from biogas slurry by NaCl- modified zeolite. *PLOS ONE* 12(5): e0176109.

Chun Hui Zhou and John Keeling (2013). Fundamental and applied research on clay minerals: From climate and environment to nanotechnology. *Applied Clay Science* 74 (2013).

Cigdem, Y.G (2010). High-rate anaerobic treatment of domestic wastewater at ambient operating temperatures: A review on benefits and drawbacks, *Journal of Environmental Science and Health*, Part A: Toxic/Hazardous Substances and Environmental Engineering, 45:10.

Daizy, P. (2010). Mangifera Indica leaf-assisted biosynthesis of well-dispersed silver nanoparticles. *Spectrochimica Acta*, Part A 78 (2011) 327–331

Dar, A. (1999). Water Quality Laboratory and Monitoring Network Study Report presented to the Department of Water Supply and Quality Control, *Federal Ministry of Water Resources, pp 1 – 60.*

Dhaval, P. & Painter, Z.Z (2017). Batch and Column Study for Treatment of Sugar Industry Effluent by using low-cost Adsorbent. Vol-3 Issue-3 2017 *IJARIIE*-ISSN(O), pp 2395-4396.

EPA, (2019b). https://www.epa.sa.gov.au/aggregation/pdf, retrieved on the 03/06/2019

Getie S., Belay A., Chandra, R.A. & Belay Z. (2017b). Synthesis and Characterizations of Zinc Oxide Nanoparticles for Antibacterial Applications. *J Nanomedic Nanotechnol* 2017, S8.

Haijiao Lu, Jingkang Wang, Marco Stoller, Ting Wang, Ying Bao, and Hongxun Hao. (2016). An Overview of Nanomaterials for Water andWastewater Treatment. *Review Article.*Hindawi Publishing CorporationAdvances in Materials Science and EngineeringVolume 2016, Article ID 4964828.

Haritha M., Meena V., Seema, C.C. & Srinivasa R.B. (2011). Synthesis and Characterization of Zinc Oxide Nanoparticles and Its Antimicrobial Activity against Bacillus Subtilis and Escherichia Coli. *Rasayan J.Chem*, Vol.4, No.1 (2011), ISSN: 0974-1496 CODEN: RJCABP, pp 217-222.

Hocaoglu, M.S., Insel, G., Ubay Cokgor, E., Baban, A., Orhon, D. (2010) COD fractionation and biodegradation kinetics of segregated domestic wastewater: black and grey water fractions. *J. Chem.Technol. Biotechnol*. 85 (9), pp 1241– 1249.

Idris-Nda, A., Aliyu, H.K. & Dalil, M. (2013), "The challenges of domestic wastewater management in Nigeria: A case study of Minna, central Nigeria", *International Journal of Development and Sustainability*, Vol. 2 No. 2, pp. 1169-1182.

Ikhazuangbe, P.M.O., Kamen, F.L., Opebiyi, S.O., Nwakaudu, M.S. & Onyelucheya, O.E.(2017). Equilibrium Isotherm, Kinetic and Thermodynamic Studies of the Adsorption of Erythrosine Dye onto Activated Carbon from Coconut Fibre. *International Journal of Advanced Engineering Research and Science (IJAERS) [Vol-4,* Issue-5, May- 2017, https://dx.doi.org/10.22161/ijaers.4.5.9 ISSN: 2349-6495(P) | 2456-1908(O),www.ijaers.com, pp 48-54.

Kuranga, I.A., Alafara A.B., Halimah, F., Fausat A.M., Mercy O.B. & Tripathy B.C. (2018). Production and Characterization of Water Treatment Coagulant from locally sourced Kaolin Clays. *J. Appl. Sci. Environ. Manage*. January, Vol. 22 (1). DOI: https://dx.doi.org/10.4314/jasem.v22i1.19, pp 103-109.

Maity, J., Sukanta P., Sourav, M., & Ratul, M. (2018). Synthesis and Characterization of ZnO Nanoparticles using Moringa Oleifera Leaf Extract: Investigation of Photocatalytic and Antibacterial Activity. *Int. J. Nanosci. Nanotechnol*., Vol. 14, No. 2, June. 2018, pp. 111-119.

Manokari.M., & Mahipal, S.S. (2016). Zinc oxide nanoparticles synthesis from *Moringa oleifera* Lam - Extracts and their characterization. *WSN* 55 (2016) EISSN 2392-2192, pp 252-262.

Marthe S., Graaff D., Hardy T., Grietje Z. & Cee,s J.N.B. (2010) Anaerobic Treatment of Concentrated Black Water in a Upflow Anaerobic Sludge Blanket (UASB) Reactor at a Short Hydraulic Retention Time (HRT), *Water* 2010, *2*, doi:10.3390/w2010101, www.mdpi.com/journal/water, pp 101-119.

Marthe S., Graaff D., Hardy T., Grietje Z. & Cee,s J.N.B. (2010) Anaerobic Treatment of Concentrated Black Water in a Upflow Anaerobic Sludge Blanket (UASB) Reactor at a Short Hydraulic Retention Time (HRT), *Water* 2010, *2*, doi:10.3390/w2010101, www.mdpi.com/journal/water, pp 101-119.

Ming H., Shujuan Z., Bingcai P., Weiming Z., Lu L. & Quanxing Z. (2012). Heavy metal removal from water/wastewater by nanosized metal oxides: A review. *Journal of Hazardous Materials* 211–212 (2012), pp 317– 331.

Muhammad, A. Shafeeq, A., Butt, M.A., Rizvi, Z. H. Chughtai M. A. and S. Rehman (2008). Decolorization And Removal of COD and BOD From Raw and BiotreatedTextile Dye Bath Effluent ThroughAdvanced Oxidation Processes (AOPS), Brazilian Journalof ChemicalEngineering, Vol. 25, No. 03, pp. 453 - 459, July - September, 2008, ISSN 0104-6632, printed in Brazil, www.abeq.org.br/bjche

Murray, H.H. (2000). Traditional and new applications for kaolin, smectite, and palygorskite: a general overview. *Applied Clay Science* 17 _2000, pp 207–221

Mutia F.H., Melati F.F., and Rositayanti H. (2020). Removal Of Bod and Cod Concentration in Wastewater Using Constructed Wetland, *International Journal of Scientific & Technology Research*, Volume 9, Issue 01, January 2020 ISSN 2277-8616 1466 IJSTR©2020 www.ijstr.org

NBS. (2017). State Disaggregated Mining and Quarrying Data. *National Bureau of Statistics*, Nigeria.

NESREA (2011). National Environmental Standards Regulations and Enforcement Agency. National Environmental (Surface and Groundwater Control) Regulations, 2011. Printed and published by the Federal Government Printer, Lagos, Nigeria. FGP71/72011/400 (OL,46), pp 1-6.

Njagi E.C., Hui.H, Lisa Stafford, Homer G., Hugo M.G., John B.C., George E.H. & Steven L.S (2010). Biosynthesis of Iron and Silver Nanoparticles at Room Temperature Using Aqueous Sorghum Bran Extracts. DOI: 10.1021/la103190n Published on Web 12/06/2010 *Langmuir* 2011, 27(1), pp 264–271.

Njagi E.C., Hui.H, Lisa Stafford, Homer G., Hugo M.G., John B.C., George E.H. & Steven L.S (2010). Biosynthesis of Iron and Silver Nanoparticles at Room Temperature Using Aqueous Sorghum Bran Extracts.

Ralf, K.i, Andreas, V., Brian S., Steffen, Z., Harald, H., Michael, B. & Hansruedi, S. (2011). Behaviour of Metallic Silver Nanoparticles in a Pilot Wastewater Treatment Plant. ACS publications, pubs.acs.org/est. dx.doi.org/10.1021/es1041892 *Environ. Sci. Technol*. 2011, 45, pp 3902–3908.

Rui M., Clément L., Jonathan D.J., Jason, M.U, Mark Durenkamp, Ben Martin, Bruce Jefferson, & Gregory Victor Lowry (2013). Fate of zinc oxide and silver nanoparticles in a pilotwastewater treatment plant and in processed biosolids. *Environ. Sci. Technol*.Downloaded from http://pubs.acs.org

Sachin K., Achyut K.P. & Singh R. K. (2013). Preparation and Characterization of Acids and Alkali Treated Kaolin Clay. *Bulletin of Chemical Reaction Engineering and Catalysis*, 8 (1), 2013, http://bcrec.undip.ac.id, pp 61 – 69.

Saikia N.J., Bharali D.J., Sengupta P., Bordoloi D., Goswamee R.L., Saikia P.C. & Borthakur P.C. (2003). Characterization, beneficiation and utilization of a kaolinite clay from Assam, India. *Applied Clay Science* 24 (2003).

ShittuK.O & Ikebana, O.(2017). Purification of simulated waste water using green synthesized silver nanoparticles of *Piliostigma Thonningii*aqueous leave extract. *Adv. Nat. Sci.: Nanosci. Nanotechnol.*

ShittuK.O & Ikebana, O.(2017). Purification of simulated waste water using green synthesized silver nanoparticles of *Piliostigma Thonningii*aqueous leave extract. *Adv. Nat. Sci.: Nanosci. Nanotechnol.*

Sierra, M.J., Adriana, P. Herrera & Karina A.O. (2018). Synthesis of Zinc Oxide Nanoparticles from Mango and Soursop Leaf Extracts.*Contemporary Engineering Sciences*, Vol. 11, 2018, no. 8.

Sierra, M.J., Adriana, P. Herrera & Karina A.O. (2018). Synthesis of Zinc Oxide Nanoparticles from Mango and Soursop Leaf Extracts.*Contemporary Engineering Sciences*, Vol. 11, 2018, no. 8.

Stoyanova A., H., Hitkova, A., Bachvarova-Nedelcheva, R., Iordanova, N.I. & Sredkova, M (2013). *Journal of Chemical Technology and Metallurgy*, 48, 2, pp 154-161.

Suhendrayatna, M., Rika A., Yuliza Fajriana, and Elvitriana (2012). Removal of Municipal Wastewater BOD, COD, and TSS by Phyto-Reduction: A Laboratory–Scale Comparison of Aquatic Plants at Different Species Typha Latifolia and

Saccharum Spontaneum *International Journal of Engineering and Innovative Technology (IJEIT)* ISSN: 2277-3754 ISO 9001:2008 Certified Volume 2, Issue 6, December 2012

Sukdeb Pal, Yu Kyung Tak, & Joon Myong Song (2007). Does the Antibacterial Activity of Silver Nanoparticles Depend on the Shape of the Nanoparticle? A Study of the Gram-Negative Bacterium Escherichia coli. *Applied and Environmental Microbiology*, Mar. 2007, Vol. 73, No. 6 0099-2240/07/$08.00_0.

Sulekha, M.S. (2016). Nanotechnology for Wastewater Treatment. *International Journal of Chemical Studies*; 4(2), Pp 22 – 24.

Sylla, A.M, Rihani J., Amine O., Assobhei, S. & Etahiri, B. (2018). Anaerobic Treatment of Black Water and the Effect of Nitrate onBioreactor Performance (RALBI), *Journal of Natural Sciences Research*, www.iiste.org, ISSN 2224-3186 (Paper) ISSN 2225-0921 (Online), Vol.8, No.7, 2018, Laboratory, Biology Department, Faculty of Science, University Chouaib Doukkali, P.O.Box 20, El Jadida 2400, Morocco.

Thabet, M. Tolaymat, A.M., El, B., Ash, G., Kirk, G., Scheckel, T.P. & Luxton, M.S. (2010). An evidence-based environmental perspective of manufactured silver nanoparticle in syntheses and applications: A systematic review and critical appraisal of peer-reviewed scientific papers. Published by *Elsevier B.V.*, doi:10.1016/j.scitotenv.2009.11.003 Science of the Total Environment 408 (2010) pp 999–1006.

Thabet, M. Tolaymat, A.M., El, B., Ash, G., Kirk, G., Scheckel, T.P. & Luxton, M.S. (2010). An evidence-based environmental perspective of manufactured silver nanoparticle in syntheses and applications: A systematic review and critical appraisal of peer-reviewed scientific papers. Published by *Elsevier B.V.*, doi:10.1016/j.scitotenv.2009.11.003 Science of the Total Environment 408 (2010) pp 999–1006

Thirunavukkarasu, R. Archana, S. Sharmila, B., Janarthanan, J. Chandrasekaran (2016). Preparation and Characterization of Zno Nanoparticles Using *Moringa Oleifera* Extract by Green Synthesis Method. *Asian Journal of Phytomedicine and Clinical Research*,www.uptodateresearchpublication.com

Thyagaraju, N. (2016). Water Pollution and its Impact on Environment of Society. *International Research Journal of Management, IT and Social Sciences*. ISSN: 2395-7492 Volume 3, Issue 5.

UN Water (2018). Sustainable Development Goal 6 Synthesis Report on Water and Sanitation Draft. Published by the *United Nations New York, New York* 10017, United States of America, www.un.org/publications, ISBN: 978-92-1-101370-2.

Vikas, S. & Akhilesh S. (2013). Nanotechnology:An Emerging Future Trend in Wastewater Treatment with its Innovative Products and Processes. *International Journal of enhanced Research in Science Technology and Engineering.* Vol.2 Issue 1, Dec – 2013, ISSN No: 2319 – 7463. pp 1 – 6.

WASH NORM (2019). Water, Sanitation and Hygiene: National Outcome Routine Mapping (WASH NORM): A Report of Findings. *Federal Ministry of Water Resources (FMWR), Government of Nigeria, National Bureau of Statistics (NBS) and UNICEF*. FCT Abuja. Nigeria.

DOI:

Wilson A.M. (2017). Crystallization of NBA-ZSM-5 from kaolin. Doctoral thesis, Department of Civil, Environmental and Natural Resources Engineering Division of Chemical Engineering, *Luleå University of Technology*

WWDR. (2017). The United Nations World Water Development Report on Wastewater – The Untapped Resource. Published in 2017 by the United Nations Educational, Scientific and Cultural Organization, 7, Place de Fontenoy, 75352 Paris 07 SP, France, *UNESCO* 2017, ISBN 978-92-3-100201-4, www.unwater.org

Yahaya S., Suzi, S.J, Nur, A.B.&Ajiya, D.A. (2017). Chemical Composition and Particle Size Analysis of Kaolin, *Path of Science*. Vol. 3, No 10 ISSN 2413-9009.

Yang Z., Yongsheng, C., Paul, W, Kiril, H. & John, C.C. (2008). Stability of commercial metal oxide nanoparticles in water. 42 (2008).

Yang Z., Yongsheng, C., Paul, W, Kiril, H. & John, C.C. (2008). Stability of commercial metal oxide nanoparticles in water. 42 (2008).

Ying C., Hao, D. & Sijia, S. (2017). Preparation and Characterization of ZnO Nanoparticles Supported on Amorphous SiO2. Nanomaterials 7, 217; doi:10.3390/nano7080217 www.mdpi.com/journal/nanomaterials